CHAPTER 4

Plasma Surface Function Groups of PLA to Inhibit Blood Plasma Protein Adsorption

4.1 General Introduction

Poly (lactic acid) (PLA) is one of the biodegradable polymers that has been increasingly important in biomedical applications, such as drug delivery, artificial tissues, implant organs, and tissue engineering [1-4] because of its biodegradability, biocompatibility and proper degradation rate compared with the healing time of the human tissues [14]. The PLA is a polymer which is made from the repeating units of monomer structure [128] as shown in Fig. 4.1.

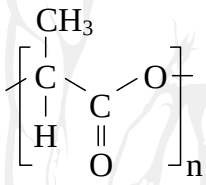

Figure 4.1 Poly (lactic acid) structure.

However, the applications in the artificial tissues and organs are limited due to limited cell attachment to the polymer surface. The reason has been attributed to the PLA-surface's hydrophobicity and lack of reactive side chain groups, but mechanisms in deeper levels have been yet unclear. Superficially seen, a more hydrophilic surface would attract more cells to attach. But, the cell attachment process is complicated, especially in the case of human cell attachment on the artificial materials. The blood plasma protein is the first to attach onto the surface material. The mechanisms of protein attach onto the surface materials depending on the surface, protein and environment, such as diffusion coefficient, molecular mass, electrical charge [129-131], polarity and pH [6, 37, 132, 133]. It is important to study different proteins adsorbed on several surfaces. In these cases, human cell adhesion was preceded by adsorption of human blood protein to the material surface. The adsorbed protein on the surface would form a

barrier layer to subsequent cell attachment; that is, the more blood protein adsorbed, the fewer cells attached. The question is then what kind of material surface the human blood protein likes to adsorb onto. In order to investigate this issue, different types of the biomedical polymer surface should be used.

Several methods have been developed to modify the surface of PLA [14, 22, 24, 132, 134]. Among them, plasma treatment is an effective method to incorporate the desired groups or chains onto the surface of the PLA [135]. Non-polymerizing gas plasma, such as CO_2, O_2, N_2, H_2, Ar, He and NH_3, can create reactive sites such as hydroxyl (-OH), carboxyl (-COOH) or amino groups ($-NH_2$) on the polymer surface [16, 36, 69, 136, 137-140]. Ammonia (NH_3) plasma was demonstrated to be able to improve the hydrophilicity and biocompatibility of PLA more effectively than other gas plasmas [69] by increasing the surface morphology, roughness and amino group while decreasing the contact angle [35, 36]. Mechanisms involved in the promotion of cell adhesion and proliferation by ammonia plasma were also studied and confirmed that wettability, chemical composition, morphology and charge of PLA were important parameters that controlled protein adsorption, cell interaction, and biocompatibility [136, 137, 141]. Recently, a number of researchers have explored surfaces that enhance specific protein adsorption or cell affinity. For example, Kunzler *et al.* [142] found that osteoblasts preferred rougher surfaces whereas fibroblasts favoured smoother surfaces. Ying *et al.* [39] showed that BSA was preferentially adsorbed onto a hydrophobic surface. They also investigated the competitive adsorption of albumin against collagen and found that albumin was adsorbed onto the hydrophobic surface better than collagen which the likes of Zhi-Hong *et al.* [143] study. Zuwei *et al.* [144] immobilize gelatin or collagen on PLLA film surfaces, poly (hydroxyethyl methacrylate) (PHEMA) or poly (methacrylic acid) (PMAA). Gelatin and collagen were reacted with the activated hydroxyl or carboxyl groups to obtain covalently immobilized protein layers. The protein immobilized PLLA improved surface wettability and biocompatible surface.

Although there have been many studies of protein adsorption onto surface of polymeric materials, a complete picture of the mechanisms has not yet been provided. When a material is inserted into a human body, protein adsorption is the first step to

take place. Albumin is the first protein adsorbed on the implant surface and then it can be replaced by immunoglobulin-G (IgG), which in turn is displaced by Fib and higher molecular weight proteins [74]. Therefore, it can correctly be said that the attachment of cells and adsorption of cell attachment proteins, in the presence of the serum, are controlled by the affinity of albumin on the surface. Therefore, in this work we, for the first time, directly used HSA, the most abundant protein in human blood plasma, and studied its adsorption on PLA surfaces, aiming at finding out relationships among the PLA surface properties which were altered by ammonia plasma treatment and adsorption of HSA for revealing relevant mechanisms in cell attachment.

4.2 Experimental Procedure

4.2.1 Sample Preparation

Films in thickness of 50 μm of PLA (NatureWork® with L/D ratios from 24:1 to 30:1) were made in the standard calendering process by the School of Mechanical Engineering, Institute of Engineering, Suranaree University of Technology, Thailand. Samples of the PLA films were prepared in 3 cm × 12 cm strips, wiped with 95% ethanol, dry by N_2 gas blowing and stored in a desiccator at 25±2ºC for 24 h prior to plasma functionalizations. Before the samples were put into the chamber, the sample was held on the sample holder. Then it was hung on the holder which was placed at the cover.

4.2.2 Plasma Treatment

Plasma functionalizations were carried out using a home-made 13.56-MHz inductively coupled plasma reactor [145], details in Chapter 3. Film samples were put into the plasma reactor which was a quartz cylinder and then the cylinder was evacuated to a base pressure of 1.4 x 10^{-2} torr. To remove residues, the film samples were first sputtered by Ar plasma at 1.0 x 10^{-1} torr and the RF power of 50 W for 30 sec. After that, the films were treated with Ar, NH_3 and Ar mix with NH_3 plasma discharged at RF powers of 50 W, 75 W, and 100 W, respectively. The gas pressure was controlled at 5.0 x 10^{-2} torr and the treatment time was fixed for 10 min.

Optical emission spectroscopy (OES) was used to observe the active plasma species. In OES the plasma radiation was collected by a lens, focused onto an optical fiber and input to a S2000 Miniature Fiber Optic Spectrometer (Ocean Optic, Inc., USA). Spectra were recorded from 200 nm to 800 nm in 0.6 nm steps.

Table 4.1 The plasma functionalizations conditions.

Conditions		Ar pre-treated		Modification	
Gas mixture		RF power (W)	Time (s)	RF power (W)	Time (min)
Ar	-	50	30	-	-
Ar	-	50	30	50	10
Ar	-	50	30	75	10
Ar	-	50	30	100	10
NH_3	-	50	30	50	10
NH_3	-	50	30	75	10
NH_3	-	50	30	100	10
NH_3	Ar 5%	50	30	75	10
NH_3	Ar 10%	50	30	75	10
NH_3	Ar 15%	50	30	75	10
NH_3	Ar 20%	50	30	75	10

4.2.3 Film Characterizations

Contact Angle and Surface Energy

Static contact angles were measured using 2-µl droplets of deionised water and diiodomethane (CH_2I_2), respectively, at room temperature. Three replications of the untreated (control) and treated films were cut into 2 cm × 4 cm. Each sample was obtained from 5 different regions. The data were collected from both sides. Images of the fluid drops were captured and analyzed by using an image analysis software. The surface energy was calculated using the Owens-Wendt equations as Eqs. 2.10-2.11.

Atomic Force Microscope: AFM

The surface morphology was observed by an AFM (SHIMADZU SPM-9500 J2, Japan). Three replications of the untreated (control), treated and protein adsorbed

PLA films were cut into 1 cm × 1 cm then put in the ample holder. Images were acquired in the tapping mode and using silicon tips with a scan rate of 2 Hz in air and a scan area size of 1μm × 1μm. Each sample was obtained from 3 different regions. The image analysis was carried out using a Di Nanoscope III version 5.12r3 software.

X-ray Photoelectron Spectroscopy: XPS

X-ray photoelectron spectra of the untreated (control), treated and protein adsorbed PLA films were obtained using an AXIS ULTRA XPS spectrometer (KRATOS analytical, UK). The monochromatic Al K_α x-ray source was operated at an anode power 150 W. Survey spectra were acquired from 0-1200 eV with pass energy of 80 eV and a step size of 1 eV. The core-level spectra (high-resolution spectra) were obtained with pass energy of 20 eV and a step size of 0.1 eV. Elemental compositions were calculated from peak areas obtained from the survey spectra. Three replications of each condition were observed. A low-energy electron flood gun was used to compensate for surface charging on the insulating films. All XPS peaks were referenced to a C_{1S} signal at a binding energy of 284.6 eV, corresponding to the C-C and C-H bonds in hydrocarbons. The peaks were deconvoluted into Gaussian components to gain the insight into the bonding with the same of the full width at haft maximum (FWHM).

4.2.4 Protein Adsorption

The HSA (lyophilized powder, A1653) and HFib (lyophilized powder, F4129) with NaCl -0.138 M, KCl - 0.0027 M in pH 7.4 at 25°C were purchased from the Sigma-Aldrich Coorporation, Germany. This HSA has a molecular weight 66,478 Da and Fib comprise of α-chain mol wt 63.5 kDa, β-chain mol wt 56 kDa, γ chain mol wt 47 kDa which soluble dimer mol wt 340 kDa. Both proteins were diluted 0.5% W/V in distilled water. Strips of untreated, treated PLA films were cut into 1 cm × 1 cm. Three replications of each condition were placed into wells of a 4-well plate. The each protein was immobilized onto the films by adding 1 ml of protein solution into each well and then the films were incubated for 20 min on a rocking shaker at room temperature. After incubation, the films were washed in distilled water for 20 min, first soaking and then rinsing 3 times. For observation and analysis of the protein adsorbed films, the films

were dried in a new plate and left at room temperature for 12 h before the AFM observation and XPS analysis. Moreover, to analyze the pure protein components, the protein solution was dropped on the 1 cm × 1 cm Si wafer and left at room temperature for 12 h before XPS analysis.

4.3 Results and Discussion

4.3.1 Plasma Diagnostics

The spectrum of NH_3 plasma was observed by OES in a range of 200-800 nm. The prominent lines observed were the NH line at 336.7 nm, the N line at 315.9 nm, the N_2 line at 357.7 nm, the N_2^+ line at 391.4 nm, the H_β line at 486.2 nm, the H_2 band at 546.0 nm, H_γ at 434.2 nm and the H_α line at 655.7 nm [146-148]. The NH, N_2, and H species increased with increasing RF power, as demonstrated in Fig. 4.2. Then adding the Ar gas into the NH_3 plasma, it was found that the spectrum of NH_3 mixed Ar plasma showed the same prominent lines with Ar line in the range of 700-800 nm. Therefore, NH_3-plasma discharged provided the nitrogen and hydrogen species. The primary decomposition process were present as below,

$$NH_3 \rightarrow NH_2 + H$$
$$NH_3 \rightarrow NH + H + H\,.$$

Moreover, the prominent species are NH and N which probable formed by the secondary decomposition process such as

$$NH_2 \rightarrow NH + H$$
$$NH \rightarrow N + H$$
$$2NH \rightarrow N_2 + H_2\,.$$

While varying the percentage of Ar gas mixture at 5, 10, 15 and 20 percent. The NH line at 336.7 nm, the N line at 315.9 and N line at 636.1 nm increased to the maximum when the Ar gas mixture was at 10 percent and then decreased since the Ar gas mixture was at 15 percent as shown in the Fig. 4.3. It seemed that the Ar gas could

be mixed in the range of 10-15 percent and would create the height associated of the NH_3 plasma.

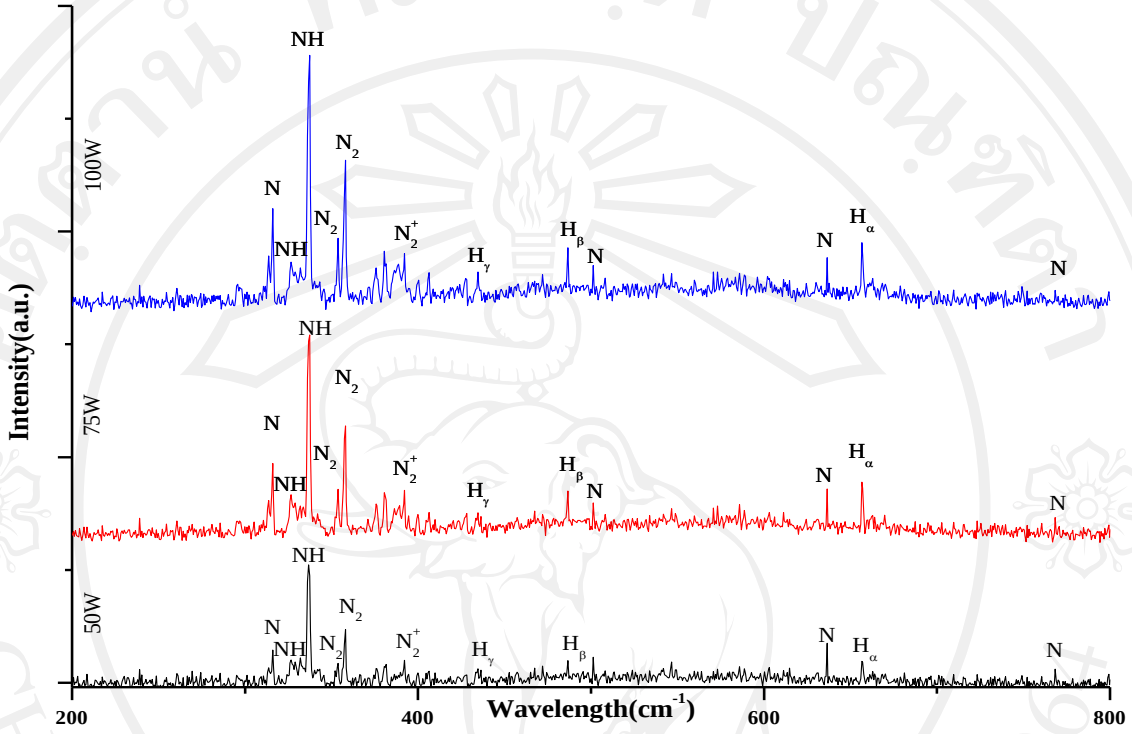

Figure 4.2 Typical optical emissions spectrum of NH_3 plasma with RF powers of 50W, 75W and 100W.

From the probability of the chemical kinetics of discharge, the collision in plasma produces the particle, excited molecule or radical with the ionization, recombination, excitation and relaxation process. Hence, the probability of the chemical kinetics of argon and ammonia discharge plasma is present as below,

$$NH_3 + Ar \rightarrow NH_2 + H + Ar$$
$$\rightarrow NH + H_2 + Ar$$
$$\rightarrow NH_3^+ + e + Ar$$
$$NH_3^+ + e \rightarrow NH_2 + H .$$

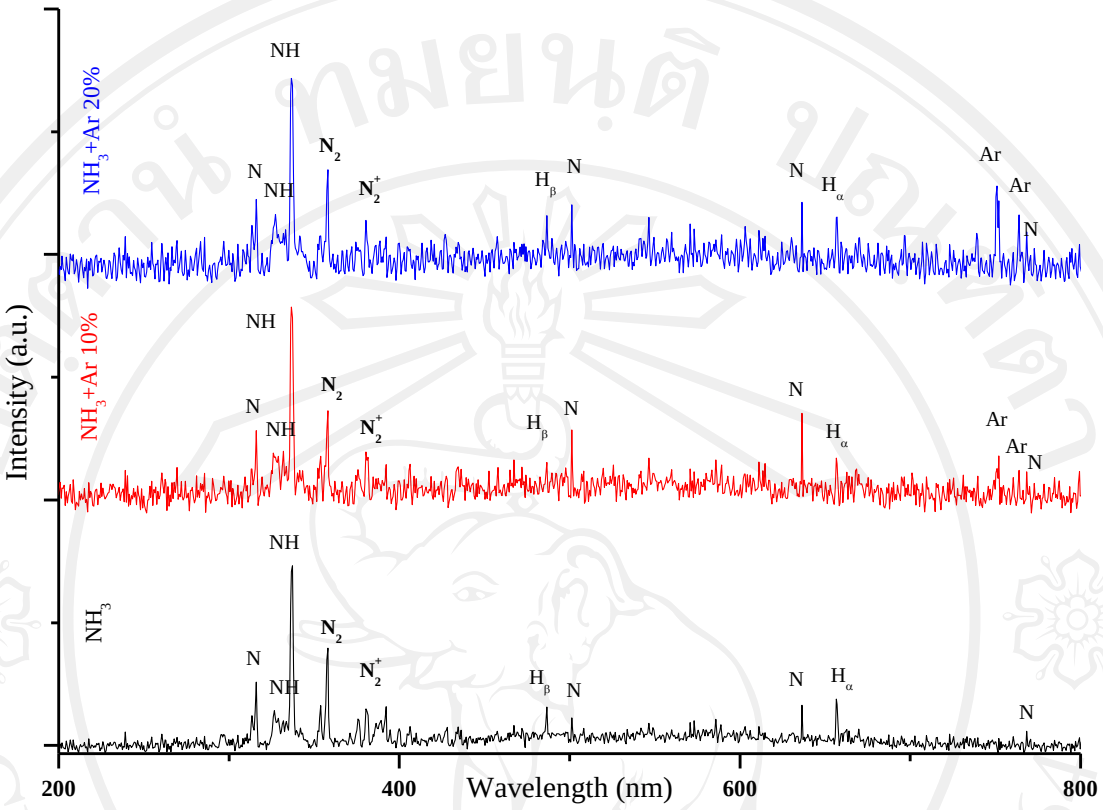

Figure 4.3 Typical optical emissions spectrum of NH_3, NH_3+Ar 10% and NH_3+Ar 20% plasma with RF powers 75W.

4.3.2 Film Characterizations

Surface Morphology

Surface morphology of the films was observed by AFM and roughness data was obtained from three different regions on each sample. Fig. 4.4 shows the AFM images of untreated, plasma treated films. AFM-measured root-mean-square (rms) roughness of the samples was in the range of 0.1-0.8 nm, as shown in Table 4.2. After Ar pre-treatment a small bump appeared. It was observed the plasma treatment caused the surface roughness and the roughness increase was little dependent on the plasma generation power. As the Ar plasma treated increases the bump on the surface. Other than, the fine grain structures of the surfaces were observed after the NH_3-plasma treatment. There were some small changes in the magnitude of the grain structure.

Additionally, the mixture gas of Ar and NH_3 plasma treatment found the fine grain structure appeared on the top of the bump surface, which appeared that the surface roughness was a result of both characteristic plasma treatments. The result on the roughness increase in agreement with a previous reported one showed the surface of PLLA became rougher form 22.32 nm to 37.50 nm after NH_3-plasma treatment with an RF power of 100 W for 2 minutes [35].

Table 4.2 The roughness of untreated PLA, Ar pre-treated, NH_3-plasma treated and Ar+NH_3-plasma treated PLA with RF powers of 50 W, 75 W and 100 W measured by AFM.

Conditions	Roughness : R_{rms}	
	(nm)	± S.D.
Untreated	0.12	0.01
Ar pre-treated	0.15	0.03
Ar 50 W	0.44	0.04
Ar 75 W	0.68	0.01
Ar 100 W	0.82	0.10
NH_3 50 W	0.25	0.01
NH_3 75 W	0.26	0.02
NH_3 100 W	0.32	0.03
NH_3+Ar 5%	0.41	0.02
NH_3+Ar 10%	0.46	0.03
NH_3+Ar 15%	0.49	0.01
NH_3+Ar 20%	0.45	0.05

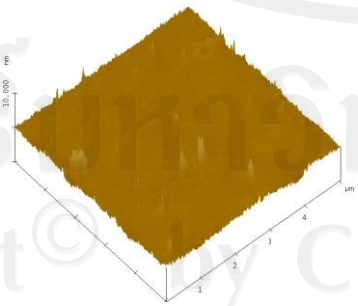

(a) Untreated

(b) NH_3 50 W

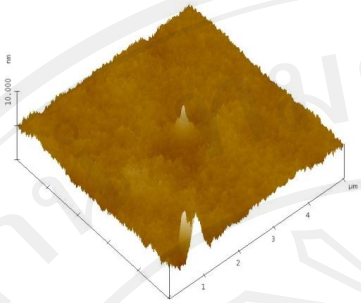

(c) NH_3 75 W

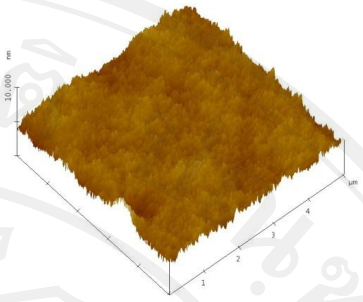

(d) NH_3 100 W

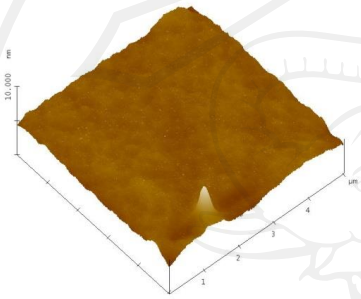

(e) Ar- pretreated

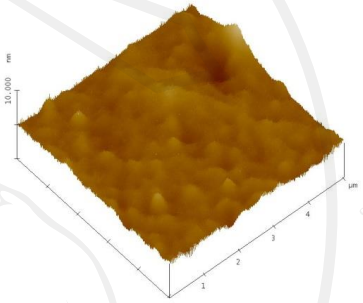

(f) Ar 50 W

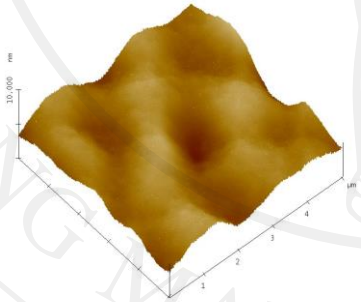

(g) Ar 75 W

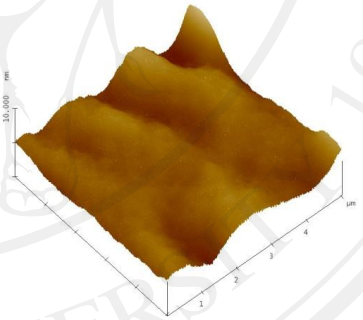

(h) Ar 100 W

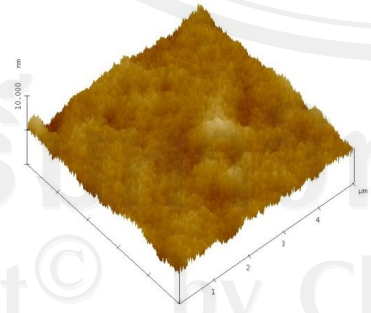

(i) NH_3+Ar 5%

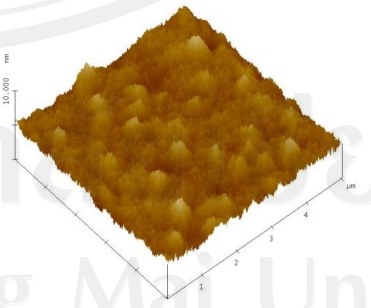

(j) NH_3+Ar 5%

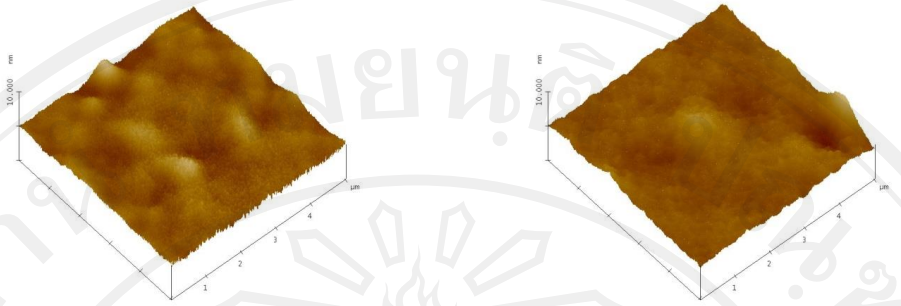

(k) NH_3+Ar 5% (l) NH_3+Ar 5%

Figure 4.4 AFM images of untreated PLA, Ar pre-treated, NH_3-plasma treated and Ar+NH_3-plasma treated PLA with various RF powers.

Contact Angle and Surface Energy

The results of the contact angle measurements as shown in Table 4.3. The water contact angle of the untreated sample was 69.0°. After Ar pre-treatment, it was found that the water contact angle decreased to 52.2° due to the changing of the surface roughness and may be the free radical from the Ar sputtering. However, only the Ar pre-treatment cannot approve the wettability of PLA. Variations of RF power of Ar treatment were studied in order to compare the effects of the Ar plasma. The Ar plasma treated shows the ability to approve wettability of the PLA films. The water contact angle decreased to 37.9°. It seems that the water contact angle decreased with increasing RF powers, and it was only a little dependent on the plasma generation power. The NH_3-plasma treatment decreased the water contact angles to 15.0°, just as the contact angles of CH_2I_2 were also decreased after the plasma treatment. In addition, the NH_3+Ar plasma treatment show the highest wettability effect of the treatment to the PLA films. The NH_3+Ar 10% plasma treatment was created the lowest water contact angle to 7.4°. Nevertheless, the 20% of Ar gas mixture to the NH_3 plasma constructs the PLA films properties similar to untreated PLA. That may be because the smooth surface and the decrease of the surface energy.

Table 4.3 also shows the components of surface energy of the samples calculated using the Owens-Wendt equations (Eqs. 2.10-2.11). The material surface

energy consists of polar and non-polar components. The polar component of surface energy comprises all other interactions due to non-London forces. Polar molecules interact with dipole forces and hydrogen bonds. The dispersive or non-polar components of surface energy result from molecular interactions due to London forces [148]. The polar components of surface energy are seen significantly increased after the plasma treatments. Although the Ar pre-treatment contributed some, it was not as much as the NH_3-plasma treatment did. On the contrary, the dispersive component decreased. The total surface energy was obviously higher after the plasma treatments, indicating that the surface of PLA became more hydrophilic.

Table 4.3 The contact angle and surface energy of untreated PLA, Ar pre-treated and NH_3 plasma treated PLA with RF powers of 50W, 75 W, and 100 W. Treatment time was 10 min.

Conditions	Contact angle (degree) ± S.D.		Surface energy (mJ/m^2)		
	θ H_2O	θ CH_2I_2	γ_s^p	γ_s^d	γ_s
Untreated	69.0 ±1.9	39.1 ± 2.0	11.0	30.3	41.3
Ar pre-treated	52.2 ±1.7	31.7 ±1.1	23.1	27.1	50.2
Ar 50 W	42.1±1.2	26.9±1.2	30.9	25.7	56.6
Ar 75 W	40.3±0.9	25.7±0.8	32.1	25.6	57.8
Ar 100 W	37.9±1.4	22.1±1.4	33.2	26.2	59.5
NH_3 50 W	20.0 ± 1.0	32.9 ± 1.9	50.4	18.2	68.6
NH_3 75 W	15.0 ± 1.0	30.3 ± 2.2	51.7	18.7	70.5
NH_3 100 W	15.5 ± 0.7	32.1 ± 1.3	52.4	18.0	70.4
NH_3+Ar 5%	11.3±1.6	26.7±1.5	51.8	19.7	71.5
NH_3+Ar 10%	7.4±0.8	25.1±1.2	52.3	20.0	72.3
NH_3+Ar 15%	21.5±1.1	28.2±1.7	47.5	20.3	67.8
NH_3+Ar 20%	32.8±1.5	27.7±1.2	22.8	39.2	61.9

However, the adding Ar gas to the NH_3-plasma treatment was more effective to corporate the polar components of surface energy to the PLA films. Decreasing the contact angle and increasing the surface energy of PLA due to NH_3 plasma treatment

were previously reported [69]. PLLA and PDLLA films decreased the average contact angle after NH_3-plasma treatment from 65-79 degrees to 21.5 degrees and increased the surface energy from 43.2 to 69.1 mJ/m^2 with increasing the contribution of the polar component (10.7 to 42.4 mJ/m^2) [69]. The hydrophilicity of the PLA films was improved by the NH_3-plasma treatment due to increased polarity groups such as amine or amide group, as there were greater polar components in the total surface energy.

The chemical compositions

The chemical compositions of the samples were analyzed and obtained from XPS. Fig. 4.5 shows the survey scans of the untreated PLA and Ar, NH_3 and NH_3+Ar plasma treatment PLA with RF powers of 75 W. The spectrum of the untreated PLA shows only C_{1s} and O_{1s} peaks as well as Ar-plasma treated, whereas N_{1s} peaks (400 eV) appeared in the spectra of the NH_3-plasma treated and all the NH_3+Ar plasma treatment samples.

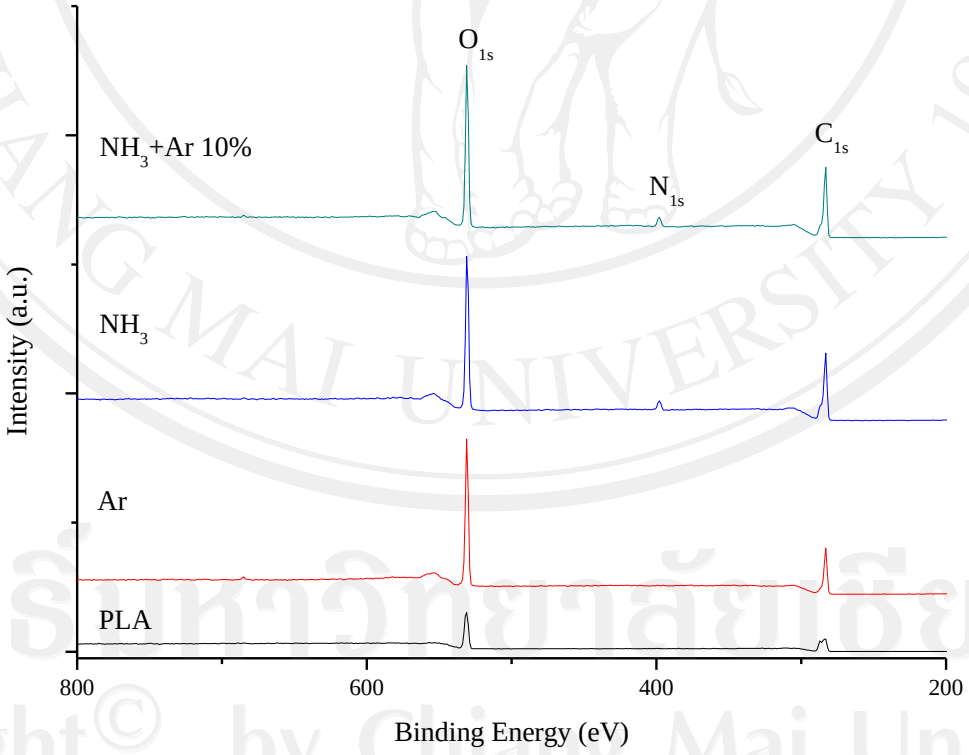

Figure 4.5 XPS survey spectra of untreated PLA and Ar, NH_3 and Ar+NH_3-plasma treated PLA with RF powers of 75 W.

The atomic compositions of C, O and N are shown in Table 4.4. While the C concentrations of the plasma-treated samples remained similar to that of the untreated sample, the O concentrations of the treated samples decreased compared with that of the untreated sample. This could be understood from the above mentioned XPS-revealed bonds, that is, nitrogen from the NH_3-plasma treatment was mainly bonded with carbon, so that carbon could be more fixed while oxygen as a gas species was more volatile. Finally, the O/C ratio decreased from about 0.60 to 0.37 and the N/C ratio increased from 0 to 0.17 when the RF power was increased from 0 to 100W. In addition, adding Ar gas into the NH_3-plasma treatment increased the N/C ratio from 0.12 to 0.13.

Table 4.4 Atomic concentrations of the chemical components of untreated PLA, Ar pre-treated, NH_3-plasma treated and Ar+NH_3-plasma treated PLA films with various RF powers.

Conditions	Atomic composition (%) ± S.D.				
	C	O	N	O/C	N/C
Untreated	62.39±0.26	37.61±0.41	-	0.603	-
Ar pre-treated	63.20±0.38	36.80±0.73	-	0.580	-
Ar 50 W	70.71±0.23	29.29±0.31	-	0.414	-
Ar 75 W	74.32±0.61	25.68±0.31	-	0.346	-
Ar 100 W	59.83±0.76	40.17±0.31	-	0.671	-
NH_3 50 W	65.41±0.66	27.43±0.96	7.15±0.22	0.419	0.109
NH_3 75 W	65.64±0.52	26.54±0.63	7.82±0.46	0.404	0.119
NH_3 100 W	65.22±0.31	23.98±0.34	10.80±0.52	0.368	0.166
NH_3+Ar 5%	62.74±0.56	29.12±0.43	8.14±0.66	0.464	0.130
NH_3+Ar 10%	65.11±0.38	26.14±0.25	8.75±0.54	0.401	0.134
NH_3+Ar 15%	65.28±0.61	26.28±0.52	8.44±0.46	0.403	0.129
NH_3+Ar 20%	60.24±0.54	32.68±0.63	7.07±0.38	0.542	0.117

However, the excess of Ar gas (at 15 to 20 percent) lead to lower dissociated of the NH_3 this related with the OES result. These results are similar to previously reported O/C ratio decrease from 0.46 to 0.34 and N/C ratio increase from 0 to 0.10

obtained also from XPS analysis [69, 149]. Decreases in O/C ratio and increases in N/C ratio could contribute to the reduction of water contact angles. N-containing groups such as the amine group were incorporated into PLA and thus contributed to the polar surface to improve the PLA wettability.

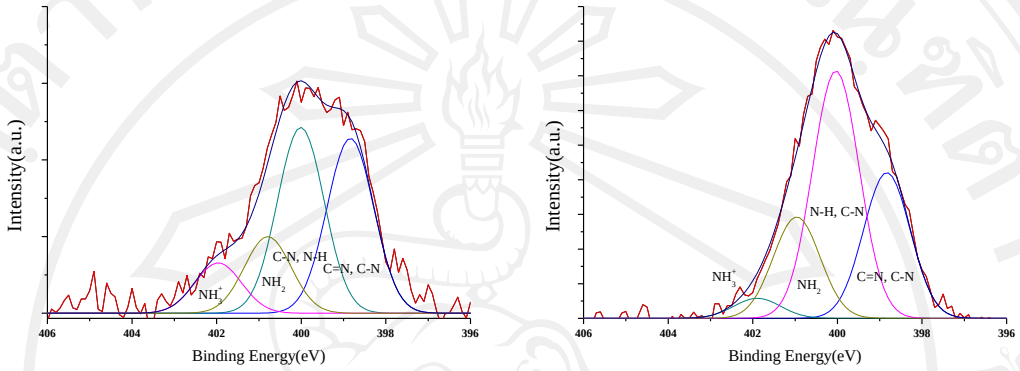

(a) (b)

Figure 4.6 Deconvoluted N_{1s} peaks of XPS spectra of NH_3 and NH_3+Ar plasma treated PLA with RF powers 75W.

To study the incorporation of N into PLA, the N_{1s} peaks of the samples were deconvoluted into several peaks, as shown in Fig. 4.6. After fitting of the N_{1s} with the same FWHM four components corresponding to nitrogen were found. The peak appearing at 398.8 eV was assigned to imine group (C=N); 399.8 eV was assigned to amine group (C-NH); 401.2 eV was assigned to amide group (C=O-NH); 402.8 eV was assigned to ammonium species (NH_3^+) [149-151]. In the group of NH_3-plasma treatment, the main component was amine group and the ammonium species was found after NH_3-plasma treatment with an RF power of 75 W and 100 W.

The C_{1s} spectrum of untreated PLA was deconvoluted into four peaks as shown in Fig. 4.7-a, 284.6 eV (C-H/ C-C), 286.6 eV (C-OH/ C-O-C), 288.9 eV (C=O/ O-C=O) and 289.7 eV (COO). The deconvoluted C_{1s} spectrum of the Ar treated samples (Fig. 4.7-b) show the promontory of C-H/ C-C peak. The deconvoluted C_{1s} spectrum of the NH_3 treated samples as shown in Fig. 4.7-c-d involves a peak at 284.6 eV associated to C-H/ C-C bonds, a peak at 286.6 eV due to C-NH and C-O bonds, a peak at 287.5 eV

due to C=O and C=N bonds, a peak at 288.2 eV attributed to C=O, HN-C=O, N-C=N bonds, and a peak at 289.7 eV owing to O=C-O(H,R) bond [149-153].

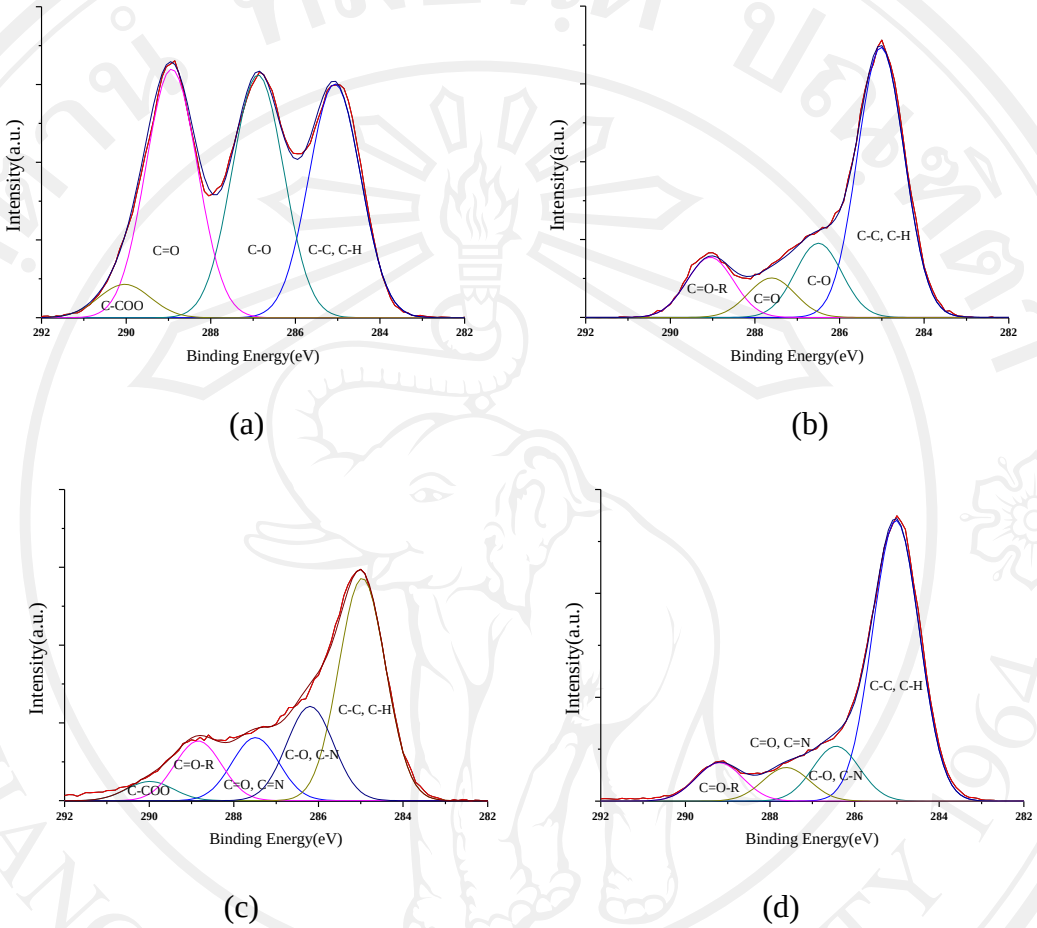

Figure 4.7 Deconvoluted C_{1s} peaks of XPS spectra of (a) untreated PLA, (b) Ar plasma treated, (c) NH_3-plasma treated and (d) NH_3+Ar-plasma treated PLA with RF powers 75W.

4.3.3 Proteins Adsorption

HSA is a heart-shaped protein with a molecular weight of 66 kDa and approximate in equilateral triangle with the dimension 3 nm × 8 nm, and it has an isoionic point of 5.5, which has a negative charge in pH 7.4 of blood [38]. AFM was used to observe the adsorption of HSA onto the surfaces of the untreated and NH_3-treated samples, as shown in Fig. 4.8-a. There was no globular structure detected by the AFM, indicating that HSA were uniformly distributed over the surface of the samples

without aggregation. The rms roughness (Table 4.5) of the HSA-covered plasma-treated samples was higher than that of the HSA-covered untreated samples and the roughness clearly increased as increasing of the RF power of the plasma generation.

Table 4.5 The root-mean-square roughness of the PLA and plasma treated films after protein-covered film samples, measure by AFM.

Conditions	Roughness (R_{rms}: nm) ± S.D. After adsorption	
	HSA	Fib
Untreated	1.27±0.07	5.97±1.38
Ar pre-treated	1.30±0.03	6.32±0.95
Ar 50 W	1.45±0.15	6.92±2.15
Ar 75 W	1.43±0.16	6.56±2.23
Ar 100 W	1.49±0.16	6.79±1.57
NH_3 50 W	1.34±0.04	8.19±2.58
NH_3 75 W	2.26±0.10	7.59±3.04
NH_3 100 W	3.10±0.08	8.96±2.19
NH_3+Ar 5%	2.80±0.13	9.25±2.02
NH_3+Ar 10%	3.29±0.06	10.47±1.94
NH_3+Ar 15%	3.14±0.06	9.56±1.06
NH_3+Ar 20%	3.00±0.10	8.86±1.71

Fig. 4.8 show the AFM roughness of untreated PLA, Ar pre-treated, NH_3-plasma treated and NH_3+Ar plasma treated PLA with RF powers 75W after HSA adsorption. The roughness of NH_3-plasma treated of RF power 75 W and 100 W were in the range of HSA size. The smoother morphology of the HSA-covered untreated sample surface was due to a higher coverage of HSA [154], whereas the coarser surface was caused by a lower HSA coverage which led to some material surface areas uncovered. From this simple observation we could see that HSA more disliked to be adsorbed on NH_3-plasma treated PLA surface.

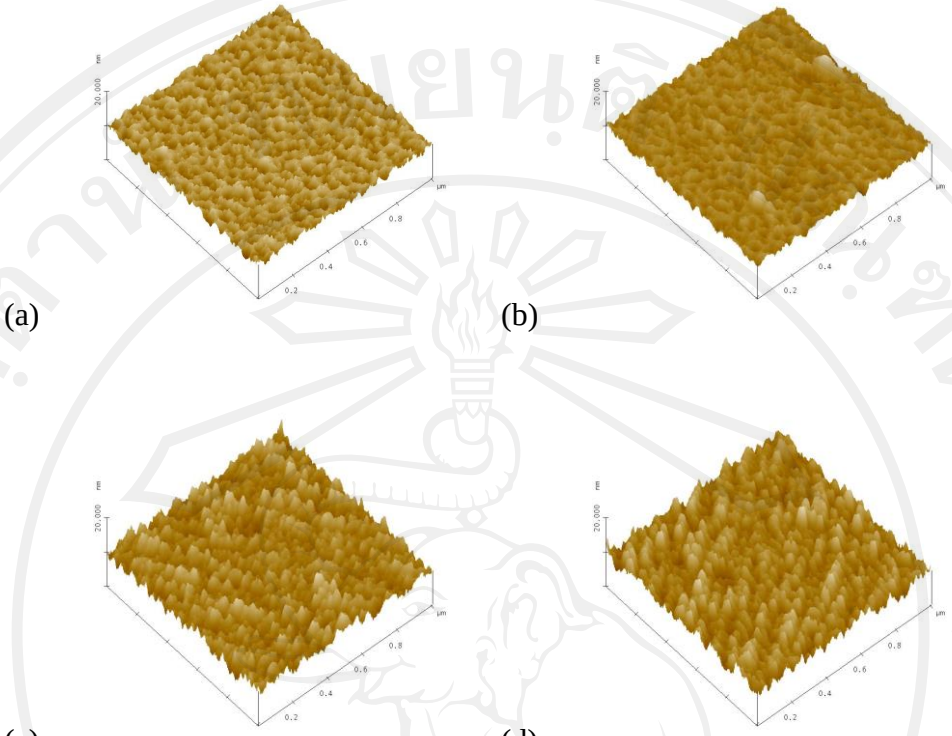

Figure 4.8 The AFM roughness of (a) untreated PLA, (b) Ar pre-treated, (c) NH_3-plasma treated and (d) NH_3+Ar plasma treated PLA with RF powers 75W after HSA adsorption.

Also Fib is elongated protein with dimension 45 nm x 9 nm x 6 nm and it is the extracellular protein with a large abundance in blood plasma. Table 4.5 shows the rms roughness of the PLA and plasma treated films before adsorption and protein-covered plasma-treated samples.

Fig. 4.9 show the AFM roughness of untreated PLA, Ar pre-treated, NH_3-plasma treated and NH_3+Ar plasma treated PLA with RF powers 75W after Fib adsorption. Fib-covered plasma-treated samples were higher than that of the HSA-covered plasma-treated samples basis the size/molecular weight. The roughness was in the range of Fib size which lies parallel down to the surface [63]. The Fib-covered sample surface tends to agree with the result of HSA. The mono layers of both proteins lie down on the surface with conformation change. The smoother morphology of the

protein covered untreated sample surface was due to a higher coverage, whereas the coarser surface was caused by a lower coverage on NH_3 plasma treated. Hence HSA and Fib disliked being adsorbed on NH_3-plasma treated PLA surface

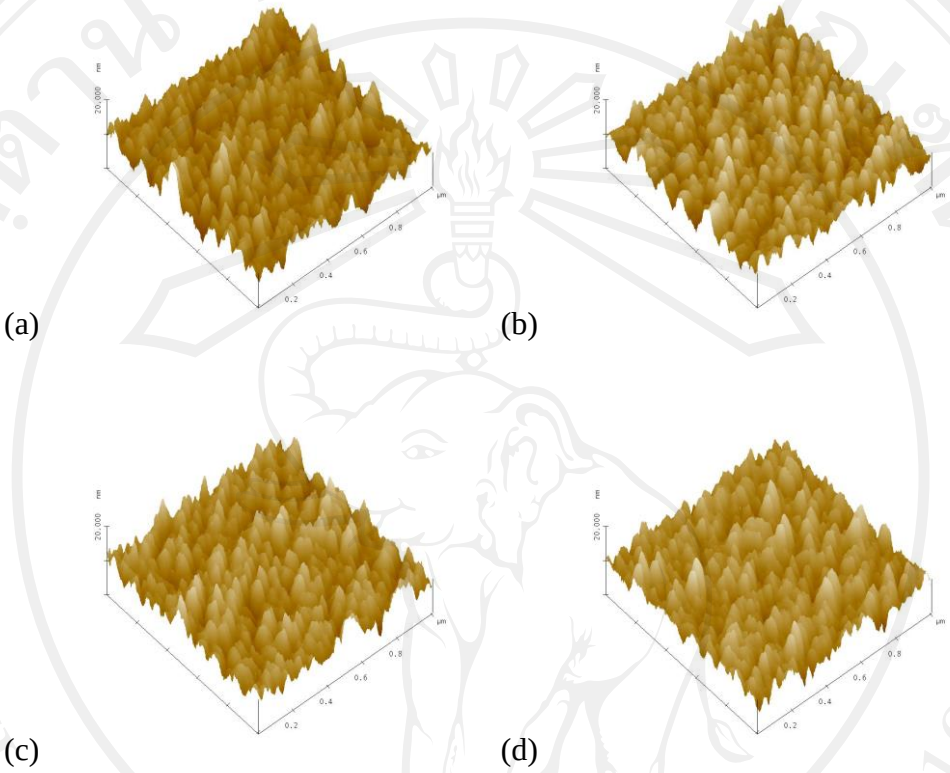

Figure 4.9 The AFM roughness of (a) untreated PLA, (b) Ar pre-treated, (c) NH_3-plasma treated and (d) NH_3+Ar plasma treated PLA with RF powers 75W after Fib adsorption.

XPS was also used to investigate the proteins attachment characteristics on the samples. In this case, the nitrogen peak appearing in the spectrum was not only caused by the NH_3-plasma treatment-introduced nitrogen but also by the presence of the amino acid sequence of the proteins molecules. The N_{1s} peak was deconvoluted into four peaks assigned to imine, amine, amide and amino groups (NH_3^+), as shown in Fig. 4.10. For pure HSA, amine group was the main structure as the plasma-treated PLA films but untreated PLA films found the main structure was imine group. The C_{1s} high resolution analysis of pure HSA (Fig. 4.11-a) show strong peaks of amino (C-NH) and peptide bound (C=O-NH). After HSA adsorption PLA film had more amide bond as NH_3-

plasma treated of RF power 50W. For NH_3-plasma treated of RF power 75 W and 100 W found decreasing in amide and amine bonding. Therefore, the HSA bounded on the surface with the carboxyl and amino groups did not interact strongly with the surface.

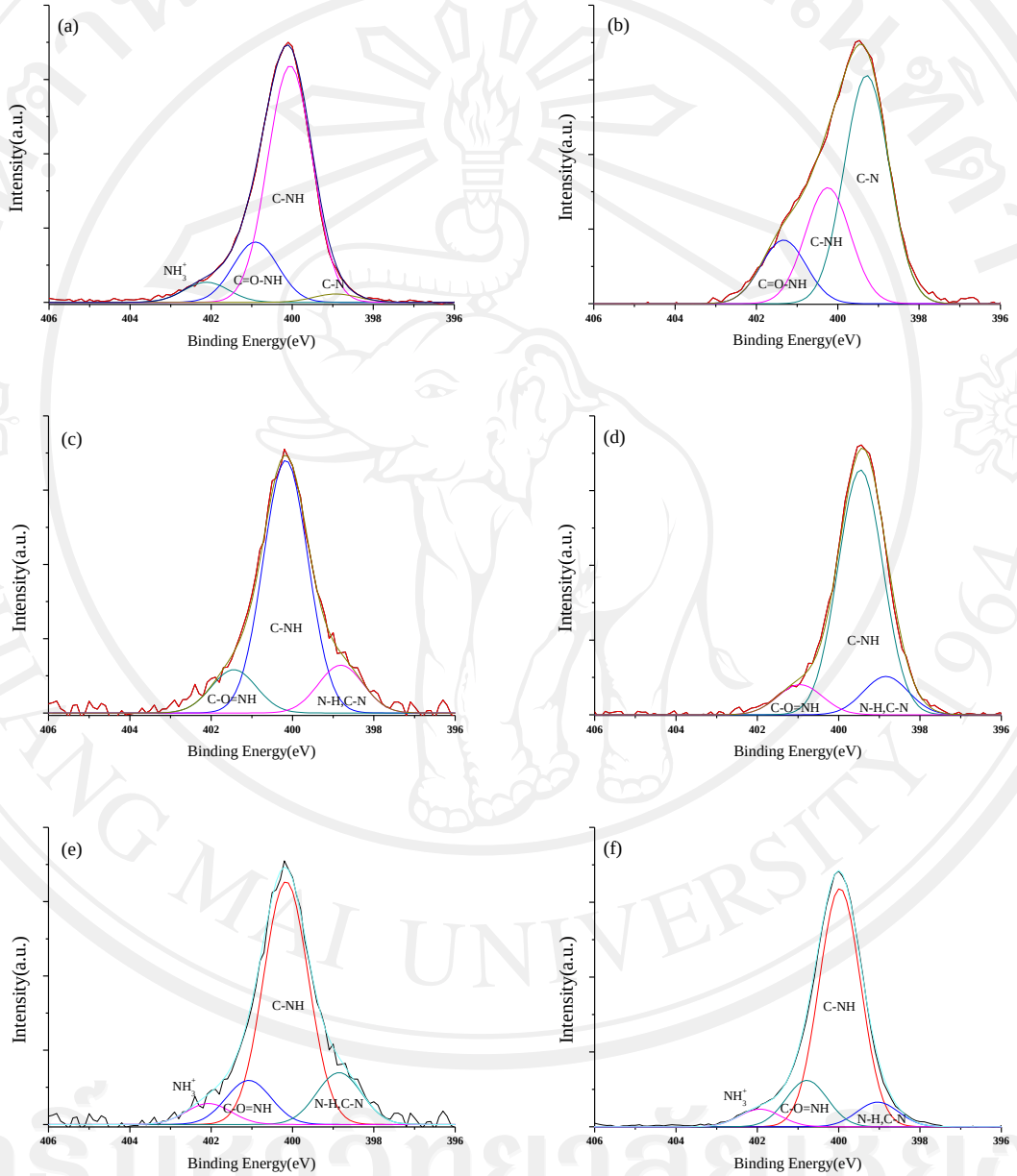

Figure 4.10 Deconvoluted N_{1s} peaks of XPS spectra of the (a) pure HSA and HSA-adsorbed on (b) untreated PLA, (c) Ar pre-treated, (d) Ar treated, (e) NH_3-plasma treated and (f) NH_3+Ar-plasma treated PLA with RF powers 75W.

Table 4.6 shows the XPS-analyzed atomic compositions of N in the untreated and treated samples after the protein adsorption. It is seen that after HSA adsorption the N concentration decreased whereas the others remained similar. Compared with the N data in Table 4.4, where the N concentration increased due to N from ammonia incorporated into PLA, the opposite trend of the N concentration change so only indicated the plasma-treated PLA adsorbed less HSA which contained nitrogen. As well as the Fib adsorption behaviours tend to be similar to the HSA adsorption. Hence, the globular and fibrous proteins have similar behaviours or mechanisms to adsorb onto the PLA.

Table 4.6 Atomic concentrations of the nitrogen components of pure HSA and protein adsorbed on untreated PLA, and plasma treated PLA analyzed by XPS.

Conditions	Nitrogen composition (%) ± S.D.	
	HSA	Fib
Pure protein	15.60±0.27	-
Untreated	8.44±0.87	15.11±0.71
Ar pre-treated	8.41±0.54	14.70±0.50
Ar 50 W	6.75±0.63	14.01±0.34
Ar 75 W	6.35±0.99	14.77±0.69
Ar 100 W	8.37±0.57	14.55±0.25
NH_3 50 W	6.49±0.26	13.67±0.75
NH_3 75 W	5.77±0.22	12.35±0.16
NH_3 100 W	3.19±0.37	12.32±1.05
NH_3+Ar 5%	5.21±0.55	12.79±0.58
NH_3+Ar 10%	3.97±0.36	11.76±0.22
NH_3+Ar 15%	5.29±0.10	13.45±0.48
NH_3+Ar 20%	5.33±0.63	13.83±0.52

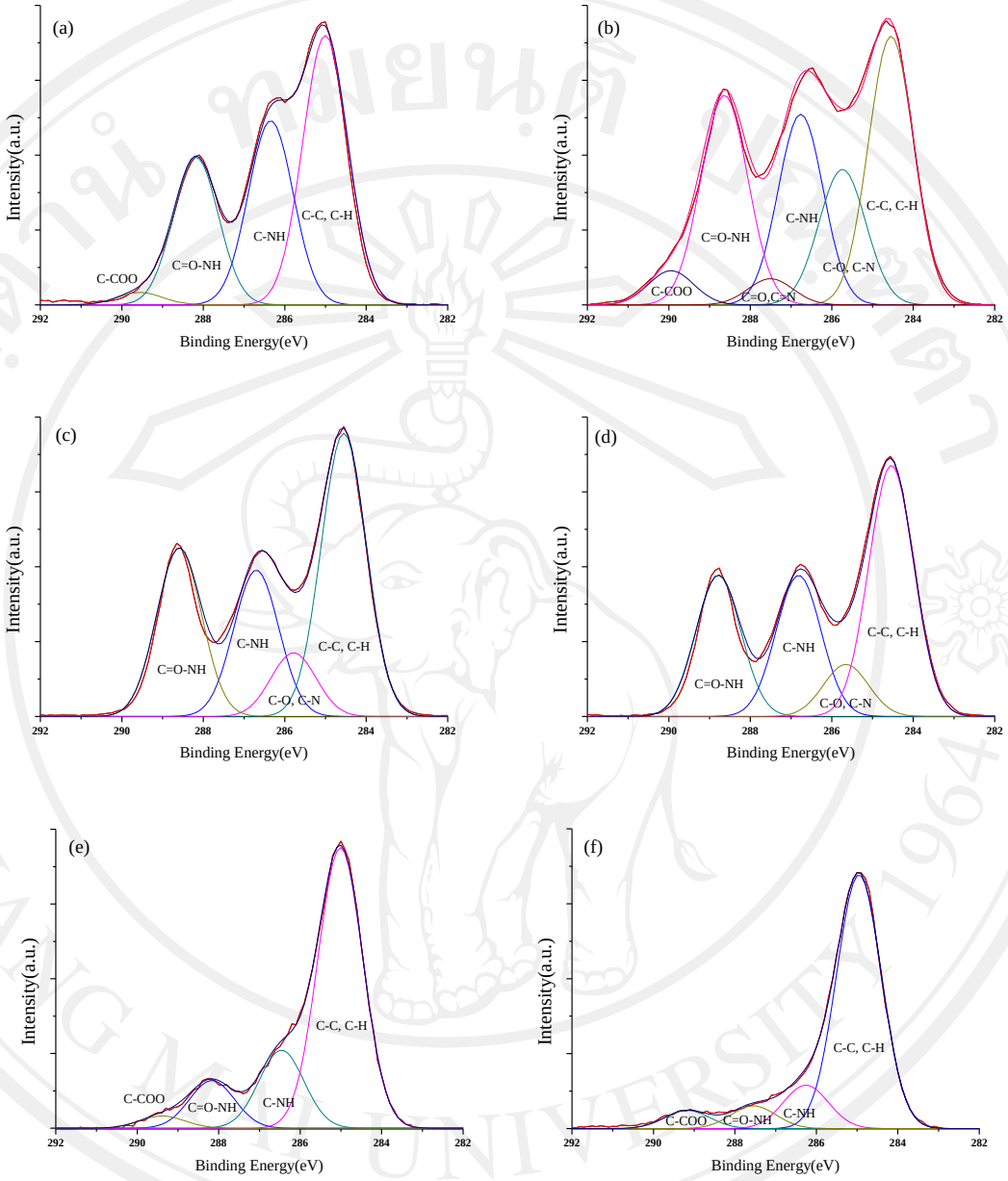

Figure 4.11 Deconvoluted C1s peaks of XPS spectra of the (a) pure HSA and HSA-adsorbed on (b) untreated PLA, (c) Ar pre-treated, (d) Ar treated, (e) NH_3-plasma treated and (f) NH_3+Ar-plasma treated PLA with RF powers 75W.

4.3.4 Discussion

All of the characterization data demonstrated that the NH_3 plasma treatment of the PLA surface resulted in an enhancement of hydrophilicity of the polymer surface from an originally more hydrophobic surface. The NH_3-plasma treatment enhances the

surface energy and hydrophilicity by increasing the roughness and introducing nitrogen and oxygen function groups onto the surface [35, 69, 149]. The protein attachment results meant that HSA and Fib were more strongly bound to the hydrophobic surface of the untreated PLA samples than to the hydrophilic PLA surface due to NH_3-plasma treatment. Normally, hydrophobic interactions are strong and thus responsible for protein attachment, whereas hydrophilic interactions with water molecules are much stronger than with proteins and hence a hydrophilic surface can hardly hold the protein [148]. In an aqueous environment, proteins tend to adopt either a hydrophobic surface or a hydrophilic surface but in different manners. Proteins can be irreversibly bound to a hydrophobic surface through the dehydration of the interface and undergoing conformation changes on hydrophobic part at the substrate surface [117]. In our case, HSA and Fib were more strongly bound to the hydrophobic surface of the untreated PLA because of dehydration during the interaction between the hydrophobic surface and blood plasma protein [155]. Thus, the HSA and Fib bound on the untreated more hydrophobic surface of PLA could not be removed by the rinsing procedure. On the other hand, HSA and Fib could be associated with the hydrophilic surface of the NH_3-treated PLA through the hydration layer and retained its original conformation. Hence, it was reversibly bound and could be washed off. As the surface had been washed with distilled water prior to XPS analysis, the protein left on the surface was considered to be irreversibly bound. The XPS analysis revealed that the polar groups containing nitrogen and oxygen were incorporated into the PLA surface to increase the surface energy of the PLA. The difference in adsorption of the proteins on hydrophobic and hydrophilic surfaces finally affects the cell attachment. HSA and Fib prefers binding to less oxygenated and more hydrophobic surfaces to form a barrier layer which thus makes subsequent cell attachment difficult. To improve cell attachment on the biomedically applied PLA, ammonia plasma treatment is then an effective choice in increasing the material surface hydrophilicity to reduce the HSA and Fib adsorption on the polymer.

4.4 Conclusion

Blood plasma proteins adsorption on the surface of biomedically applied PLA was investigated for understanding mechanisms involved in cell attachment on the

polymer and eventually looking for a solution to limited cell attachment on the polymer. Two types of PLA surfaces were tested, i.e. originally untreated PLA and NH_3-plasma treated PLA. HSA and Fib were adsorbed less on the plasma-treated PLA but more on the untreated PLA. The material characterizations demonstrated that NH_3-plasma treatment raised the surface hydrophilicity of the PLA films due to the polar groups such as amines or amides. The HSA and Fib have a higher adsorption preference to non-polar surfaces than polar surfaces. The results of this study argued that polarity influences the protein adsorption. The hydrophilic surface of PLA, induced by NH_3 plasma, would benefit to cell adhesion and enhance cell attachment since albumin was loosely bound on the surface and could thus be replaced by larger cell attachment proteins such as fibronectin, vitronectin and collagen which are the components of the extracellular matrix.